Journal of Macromolecular Science, Part A
Publication details, including instructions for authors and subscription information:
http://www.informaworld.com/smpp/title~content=t713597274

Study on the Effect of Nano and Active Particles of Alumina on Natural Rubber-Alumina Composites in the Presence of Epoxidized Natural Rubber as Compatibilizer

B. B. Konar[a]; S. K. Roy[a]; T. K. Pariya[b]
[a] Department of Polymer Science and Technology, University of Calcutta, Kolkatta, India [b] Department of Chemical Technology (Ceramic Engineering Division), University of Calcutta, Kolkatta, India

To cite this Article Konar, B. B. , Roy, S. K. and Pariya, T. K.(2010) 'Study on the Effect of Nano and Active Particles of Alumina on Natural Rubber-Alumina Composites in the Presence of Epoxidized Natural Rubber as Compatibilizer', Journal of Macromolecular Science, Part A, 47: 5, 416 — 422

To link to this Article: DOI: 10.1080/10601321003659531

URL: http://dx.doi.org/10.1080/10601321003659531

Journal of Macromolecular Science, Part A: Pure and Applied Chemistry (2010) **47**, 416–422
Copyright © Taylor & Francis Group, LLC
ISSN: 1060-1325 print / 1520-5738 online
DOI: 10.1080/10601321003659531

Study on the Effect of Nano and Active Particles of Alumina on Natural Rubber–Alumina Composites in the Presence of Epoxidized Natural Rubber as Compatibilizer

B. B. KONAR[1,*], S. K. ROY[1] and T. K. PARIYA[2]

[1]*Department of Polymer Science and Technology, University of Calcutta, Kolkatta, India*
[2]*Department of Chemical Technology (Ceramic Engineering Division), University of Calcutta, Kolkatta, India*

Received August 2009, Accepted October 2009

Natural rubber composites with alumina of different particle sizes (28 nm nano particles, 200 nm active particles and > 1000 nm raw alumina) were prepared by the usual rubber processing technique. Epoxidized natural rubber (ENR) was used in the composites as compatibilizer. Cure characteristics and mechanical properties of all composites were analyzed. The values of minimum rheometric torque (M_L), maximum rheometric torque (M_H) and torque difference ($M_H - M_L$) increased. Maximum enhancement was observed for the nano-filled composites. It endorses the view that nano alumina reveals highest interaction with natural rubber in presence of ENR. Scorch time and optimum cure time values for nano-composites were highest among all types of composites. Vulcanization reaction for the sulfur curing system of the composites was found to follow first order rate kinetics. Specific rate constant decreased with decreasing particle size in composites. Crosslink densities of composite-vulcanizates showed increasing trend with decreasing particle size of alumina. Mechanical properties of the composite vulcanizates increased with decreasing particle size of alumina - nano composites exhibiting much higher mechanical strength. Results of oxidative resistance reveal that particle size of alumina in composite vulcanizates has a significant impact on aging behavior.

Keywords: Alumina, nano particle, active particle, crosslink density, aging

1 Introduction

Inorganic materials in polymer composites are well known for reinforcement of polymers. In the development of nano-filled polymer composites, nanoscopic inorganic particles (typically 10–100°A in at least one dimension) are dispersed in an organic polymer matrix. Rubber - nano particle composites play a very important role in rubber technology and material engineering. Zhang (1) used nano magnesium hydroxide powder for fire resistance EPDM composites. Wang studied natural rubber- clay (montmorillonite) composites (2). Mishra (3) synthesized nano calcium carbonate by *in situ* deposition technique. Gilbert (4) developed epoxy-based film adhesives with nano alumina. Precipitated amorphous silica was proven to be the filler for manufacture of high performance pneumatic passenger car tires (5). However, improvements were affected only when silica was incorporated into S-SBR (sulfur – styrene -butadiene rubber) with silica coupling agent.

Alumina is one of the most widely used advanced ceramic structural materials. Active (calcined) and nano alumina were synthesized by solvothermal technique (6). Nano size alumina powder was found to have a size of 28 nm, while active alumina a crystallite size of 200 nm. Crystal structure of alumina exhibits atom planes parallel to basal plane (7). Nano alumina is similar in size with rubber reinforcing carbon black (eg. ISAF, HAF etc.). Viscoelastic properties of vulcanized rubber- high density metal oxide composites improves wet traction, rolling resistance etc., which are key factors in tire technology (5).

Aging of rubber vulcanizates depends primarily on the type (mono, di, poly, cyclic etc.) and degree of crosslinks (8). Some other ingredients like fillers, antioxidants also influence the aging behavior. Alumina is heat-resistant inorganic filler. Therefore, evaluation of oxidation characteristics of alumina filler loaded vulcanized sample is very important. Ceramic materials can be more easily dispersed in polar polymers like nitrile rubber, silicone rubber etc. Teh (9) suggested ENR (epoxidized natural rubber) as a compatibilizer for natural rubber–organoclay nano composites.

In the present work we have tried to confine our attention in three types of alumina, large particle size (above 1000 nm) raw alumina, calcined alumina (200 nm) and

---

*Address correspondence to: B. B. Konar, Department of Polymer Science and Technology, University of Calcutta, Kolkatta 700009, India. E-mail: bidyutbarank@yahoo.com

Table 1. Basic recipe of the mixes

Ingredients	*Mix G (Without Alumina, Gum compound)*	*Mix A (Composite)*	*Mix B (Composite)*	*Mix C (Composite)*	*Mix D (Composite)*	*Mix E (Composite)*	*Mix F (Composite)*
Natural rubber (RMA1X)	100.0	100.0	100.0	100.0	100.0	100.0	100.0
Zinc oxide	5.0	5.0	5.0	5.0	5.0	5.0	5.0
Stearic acid	1.5	1.5	1.5	1.5	1.5	1.5	1.5
IPPD[a]	0.5	0.5	0.5	0.5	0.5	0.5	0.5
Sulfur	2.0	2.0	2.0	2.0	2.0	2.0	2.0
CBS[b]	1.2	1.2	1.2	1.2	1.2	1.2	1.2
MBT[c]	0.8	0.8	0.8	0.8	0.8	0.8	0.8
Raw[d] Alumina	—	20	40	60	—	—	—
Active[e] Alumina	—	—	—	—	20	40	—
Nano[f] Alumina	—	—	—	—	—	—	20
ENR-50[g]	—	10	10	10	10	10	10

[a] N-isopropyl-N-phenyl-p-phenylenediamine.
[b] N-cyclohexyl benzthiazyl sulphenamide.
[c] 2-mercaptobenzthiozole.
[d] Product of heating $Al(OH)_3$ at 200°C (boehmite as well as bibbsite forms), 350 nm particle size.
[e] Alumina having crystallite size of 200 nm.
[f] Alumina having crystallite size of 28 nm.
[g] Epoxidized natural rubber (50%).

nano alumina (28 nm), to evaluate their comparative characteristics as a filler on natural rubber–alumina composites in the presence of epoxidized natural rubber (ENR) as compatibilizer.

2 Experimental

2.1 Materials

In the experiment, the amount (parts per hundred parts of rubber, phr) of different alumina was varied: for raw alumina 20,40 and 60 , for active alumina 20 and 40, for nano alumina 20 phr. Rubber and other ingredients were kept constant for all recipes (Table 1).

Natural rubber (Mooney viscosity ($ML_{(1+4)}$) 72 at 100°C) was obtained from Kerala Rubber Board, India. ENR-50 (53% epoxidization) was supplied by Malaysian Rubber Board.

Zinc oxide (99%), stearic acid, CBS, MBT, and IPPD were procured from local market. All grades of alumina were prepared and characterized in the authors' laboratories.

2.1.1. *Mixing of the ingredients*

All unvulcanized rubber mixes were prepared using a Brabender machine (Plastograph Electronical Torque Rheometer, Type815606, made in Germany) according to ASTM D-3192, working at 70°C (cold mastication and mixing) and a rotor speed of 60 rpm for 8–10 min. Except sulfur, all ingredients were mixed in it. Finally, sulfur was mixed on a laboratory size two-roll mill (30 × 15 cm) following ASTM D-3185-88.

2.1.2. *Cure characteristics*

From the matured unvulcanized stocks, samples were taken for testing cure characteristics using a Monsanto ODR100 at 150°C with a micro-die and 3° arc of oscillation.

2.1.3. *Vulcanized sheets preparation*

Vulcanization of stock samples was carried out on a three-piece preheated die placed on 46 cm × 46 cm.platens using an electrically heated press maintained at 150°C and 45 kg/cm^2. Cure sheets of approximately 2–3 mm thickness were prepared.

2.1.4. *Swelling characteristics and crosslink density measurement*

For each vulcanized sheets, the value of M_c (mean chain segment molecular weight) was calculated by measuring equilibrium swelling volume in benzene and with the help of quantitative expression of the Flory–Rehner equation (10),

$$\rho V_s V_r^{1/3}/M_c = -[\ln(1 - V_r) + V_r + \chi {V_r}^2]$$

where ρ, density of rubber; V_s, molar volume of solvent; V_r, volume fraction of rubber in swollen gel; χ, interaction parameter for rubber- solvent system. $1/M_c$ is the crosslink density of the vulcanizate.

2.2 Mechanical Properties

Tensile stress-stain properties were carried out according to ISO-37 using dumb-bell specimens at 25 ± 2°C. Test samples were punched from the vulcanized sheets parallel to the grain directions using a dumb-bell die (9C-type).

Table 2. Cure characteristics (ODR. 30 min at 150°C, 3° Arc)

Rheomatric result	*G (Gum)*	*A*	*B*	*C*	*D*	*E*	*F*
Torque,Min(M_L),N.m	5.5	10.0	12.0	13.0	13.0	15.0	20.0
Torque,Max(M_H),N.m	41.0	51.0	51.0	51.0	60.0	60.0	70.0
Tor.Diff(M_H-M_L),N.m	35.5	41.0	39.0	38.0	45.0	45.0	50.0
Scorch time, min	0.92	1.38	1.40	1.40	2.00	2.15	2.00
Optimum cure time (min)	4.25	5.00	5.00	5.25	6.30	6.75	6.50
Specific rate constant (k_1)	1.41	0.95	0.96	0.95	0.82	0.82	0.80

Thickness of the sample was measured by bench thickness gauge. Samples were tested in an Universal testing machine (UTM LR 10K PLUS, LLOYD Instrument Ltd., Hemetek Techno Instrument, Inc.) at a crosshead speed of 50 cm/min. Modulus (load at 300% elongation) was recorded and elongation at break was measured. Shore A Durometer was used to evaluate hardness of the vulcanizates as per IS 3400. An air oxidative aging test was performed in an air-circulating oven with dumb-bell specimens according to ASTM D2084 at 100 ± 2°C.

3 Results and Discussion

3.1 Cure Characteristics

Table 2 depicts the cure characteristics of rubber–alumina composites. The results show that addition of alumina increases M_L,M_H, as well as M_H–M_L in all the composites. Maximum values are found for nano composite. In presence of ENR, all types of alumina show interactions with natural rubber. Highest compatibility is experienced for nano particles. Active alumina composites show moderate results. The results are in tune with those of Teh (9) regarding ENR as compatibilizer.

3.2 Minimum Torque (M_L)

M_L expresses viscosity of rubber compounds. In the present study, viscosity increases with a decrease in the filler size. This may be due to increasing flow resistance caused by smaller sized alumina particles. In effect, it increasingly restricts the molecular motion of macromolecules (11).

3.3 Maximum Torque (M_H)

M_H indicates vulcanizate strength of rubber compounds. Adequate filler surface wetting and strong filler particle interaction with neighboring polymer molecules in the network is the cause for higher M_H. Spreading of polymer chain segments has been shown to be more as filler surface increases (12). Hence, the nano composite shows maximum torque.

3.4 Difference of Torque Values (M_H–M_L)

The extent of vulcanization and attainment of characteristics network chains relate to the change of torque value (M_H–M_L). Distribution of filler particles in rubber matrix depends on particle size. Distribution of filler influences crosslink density and Van der Walls force of attraction (physical crosslink). The present results of nano and other aluminas are in conformity with theoretical aspects.

3.5 Scorch Time and Optimum Cure Time

Table 2 shows the scorch and optimum cure time of the composites. Both the properties of filler-loaded composites are higher than the gum (without filler) compound. These properties are generally related to nature of curing system [accelerator(s), sulfur- accelerator ratio], nature of rubber and temperature of the measurement. In some cases, nature (acidic/basic) and size of filler (as for example, carbon black) affect these properties (11). In the present experiment, alumina slows down crosslink formation during vulcanization. Nano (the smallest size) composite gives longest scorch delay and largest optimum cure time. Active filler behaves similar to nano filler. In the combined accelerator systems, different ligands normally arising from different accelerators may interact with each other with the common objectives of polysulfide formation (13). It is assumed that alumina creates hindrance to this interaction due to its insolubility in rubber. According to reports (14,15), zinc oxide increases the rate of formation of polysulfide, because its coordinate complexes are soluble in rubber.

3.6 Kinetics of Vulcanization

According to kinetics of vulcanization of rubber compound (16),

$$\ln[(R_\infty - R_t)/(R_\infty - R_0)] = k_t(t - t_i)$$

where R_∞ is the difference of maximum and minimum torque (M_H–M_L), R_t the difference of torque at any time ‘t’ and minimum torque (M_t–M_L), R_0 is M_L, k_1 the specific cure rate constant and t_i the delay time.

Plots of ln [(R_∞- R_t)/(R_∞-R_0)] vs. cure time (t) at 150°C for alumina–rubber composites are shown in Figure 1. Plots are almost linear, indicating that sulfur curing with CBS-MBT accelerated alumina rubber composites is first order.

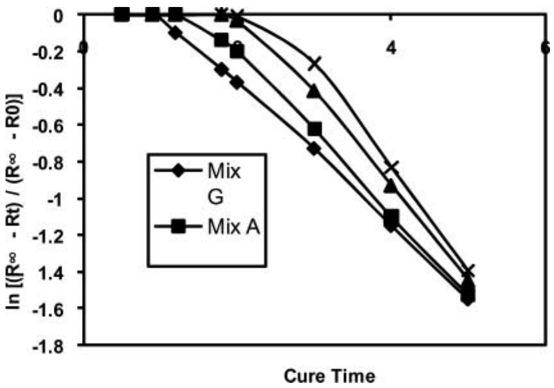

Fig. 1. Plots of ln [$(R_\infty - R_t)/(R_\infty - R_0)$] vs. cure time for sulfur cured alumina–rubber.

Table 3. Swelling and crosslink density

Sample	*V_r = Volume of unswelled rubber/ Volume of swollen rubber gel (V_r is volume fraction of rubber)*	*$V_{r(Gum)}$ / $V_{r(Filler)}$*	*$1/M_c \times 10^{-4}$*
MixG,gum	0.1984	—	1.231
Mix A	0.2702	0.7342	2.541
Mix B	0.2605	0.7616	2.504
Mix C	0.2299	0.8629	2.132
Mix D	0.2950	0.6725	3.259
Mix E	0.2910	0.6817	3.216
Mix F	0.4739	0.4186	11.099

However, k_1(the first order specific rate constant) is not the same for all composites (Table 2). Analogous results were obtained for natural rubber gum stock using TBBS accelerator (17). But it was shown that kinetics of blend accelerator systems were initially first order, and higher order at the later stage of vulcanization. The present results are not in agreement with the aforesaid report for both gum and filled stocks.

Electronic configuration of valence shell of aluminium is $3s^2 3p^1$. Therefore, aluminium should exhibit +1 and +3 oxidation state. For its small size, it has a tendency to form complexes where central atom aluminum achieves coordination number 6 by using vacant p and d orbitals. So, loosely bound unstable monovalent (absence of inert pair effect) and stable trivalent aluminium can form complexes with different ligands (18) normally generated from different accelerators. This can be compared with de Boer's concept of mobile adsorption (19). As a result, the objective of polysulfides formation is delayed. So the state of crosslink formation is slowed down. Kinetic results (lowering of specific rate constant) clearly indicate this phenomenon. Small size nano alumina shows maximum effect. CBS is a delayed action accelerator and MBT is semi ultra. In the present study, alumina filled combined accelerators stocks indicate further delay. Hence, these stocks have no deterioration in prolong storage under tropical conditions and are very safe stocks at processing temperature.

3.7 Crosslink Density

The higher the crosslink density of rubber composite,the lower the swelling of the vulcanized in a given solvent. Results of vulcanized alumina–rubber composites are shown in Table 3. Lower volume fraction in swollen gel (V_r) indicates a low crosslink density in vulcanized rubber. From Table 3, it is clear that any type of alumina filler used in composite increases crosslink density ($1/M_c$) with respect to gum vulcanizate. There has been a report related to filler effect on crosslink density (20). An additional crosslink concept (different from chemical crosslinks) consisting of sulfur bridges was also mentioned (21). It is also similar to the concept of mobile adsorption. In the present work, it is observed that binary accelerator system of CBS with booster MBT gives satisfactory results with regard to speed at the vulcanization temperature (150°C). This is reflected in the results of crosslink density.

Swelling takes place only when the osmotic pressure exerted on the rubber by the solvent is stronger than the cohesive forces of the molecules of the rubber. Osmotic pressure exerted on the rubber by the solvent falls as the molecular weight of the rubber increases with cross-linking (22). For raw alumina, crosslink density decreases to some extent with increase in loading. This may be due to a dilution effect and agglomeration of the filler particles. For active alumina, there is no significant change of crosslink density with an increase of loading. A remarkable result is observed for nano alumina filled rubber composite. This may be attributed to extensive (molecular level) distribution of filler in the rubber matrix. It causes less imperfections or flaws. It was reported that short-network chains experience abnormally high stress because of finite extensibility (23). Therefore, an increase of effective crosslink density is a consequence of small size filler effect and of the topologically

Table 4. Mechanical properties of different types of alumina filled natural rubber composites

Properties	*Mix G*	*Mix A*	*Mix B*	*Mix C*	*Mix D*	*Mix E*	*Mix F*
Modulus at 300% elongation (kg/cm^2)	12.43	17.15	14.25	10.20	20.84	18.79	30.75
Ultimate Tensile Strength (kg/cm^2)	57.16	59.01	49.01	45.29	78.46	75.51	165.58
Elongation at Break (%)	800	478	450	402	500	490	633
Hardness (Shore A)	50	50	52	54	51	53	58

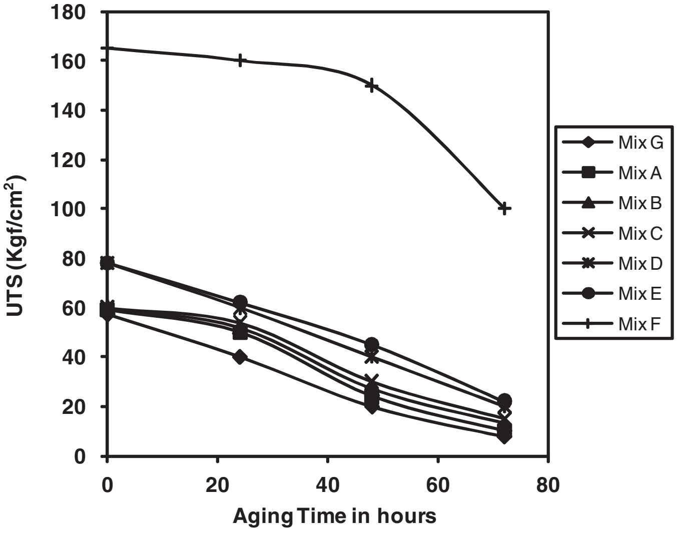

Fig. 2. Plots of Ultimate tensile strength (UTS) vs. aging time of S/CBS/MBT cured alumina.

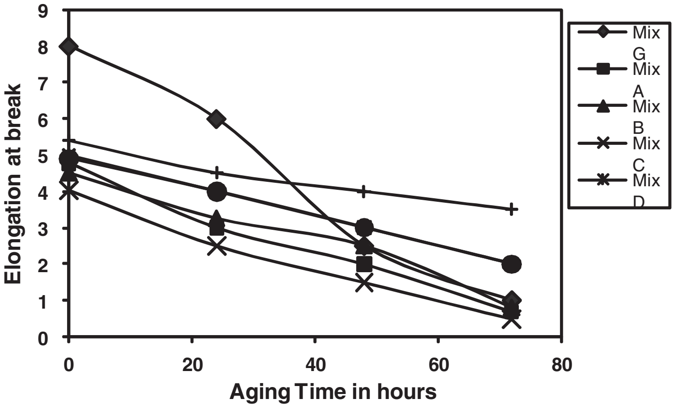

Fig. 3. Plots of Elongation at break (EB) vs. aging time of S/CBS/MBT cured alumina.

permanent entanglements arising from anchoring of rubber chain ends (24).

3.8 Mechanical Properties

Table 4 summarizes mechanical properties of unfilled and filled alumina rubber composites. Modulus, ultimate tensile strength and hardness show similar increasing trend as crosslink density. Elongation at break (EB) % decreases with filler loading. Distribution of filler is very important for mechanical properties of rubber-filler composites (25). Adequate distribution of large size particles is very difficult. Moreover, agglomeration of filler particles creates weak zone (filler – filler cohesion) in composites (26). Higher filler loading increases number of such weak zones. This explains decreasing trend with increasing filler loading. A comparatively low amount and molecular level mixing capabilities of nano filler effect lower extent of agglomeration and strong filler-rubber interaction in the composites.

Previous study (27) about the shape of alumina particles indicates that active alumina is an almost round shaped small crystalline structure with a surface area of 10.22 m^2/g, whereas the nano alumina has plate structure (one dimension is much smaller than the other two) with larger surface area of 85 m^2/g. Hence, anisometry experienced the minimum for active alumina filler composite and maximum for nano filler composite. The strength of filler-rubber composites increases with increasing anisometry (28). Therefore, nano alumina-filler geometry is an important factor for tremendous improvement of mechanical properties. High crosslink density and optimum cure characteristics at vulcanization temperature also support this aspect. An increase in hardness is related to reinforcement, amount and type of filler. The present values of hardness are in good agreement with the combinatorial effect of the above factors.

3.9 Oxidative Aging of Gum and Alumina Filled Vulcanizates of Natural Rubber

Figures 2 and 3 show the results of aging on ultimate tensile strength (UTS) and elongation at break (EB) of gum and alumina filled vulcanized samples. Aging significantly reduces stress and strain. The nano alumin-filled vulcanized sample shows much higher aging resistance than gum and other alumina filled stocks. Nono-alumina filler specimen aged for up to about 48 h resists degradation. It is almost the same as the original sample. The ratio of UTS of the aged specimen to the initial value (i.e. relative tensile strength) and relative strain to break up to 3 days /72 h of aging for gum and filled composites are shown in Figures 4 and 5. During an initial aging period of 24 h, relative tensile strength and relative strain to break for gum and filled samples are reduced in a similar way. For further aging of 48 h, relative strain to break for gum becomes the lowest and for nano-alumina the highest. One possible explanation

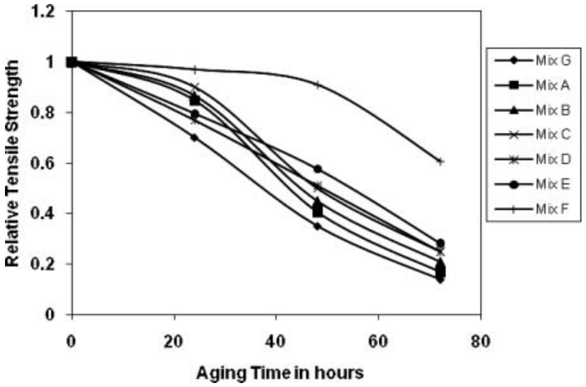

Fig. 4. Plots of Relative Tensile strength vs. aging time of S/CBS/MBT cured alumina.

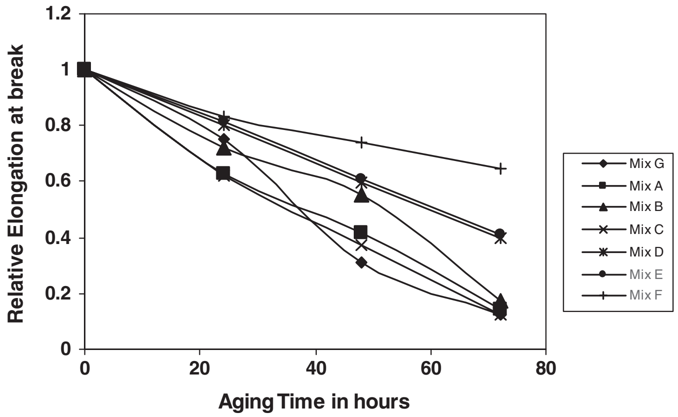

Fig. 5. Plots of relative elongation at break vs. aging time of S/CBS/MBT cured alumina.

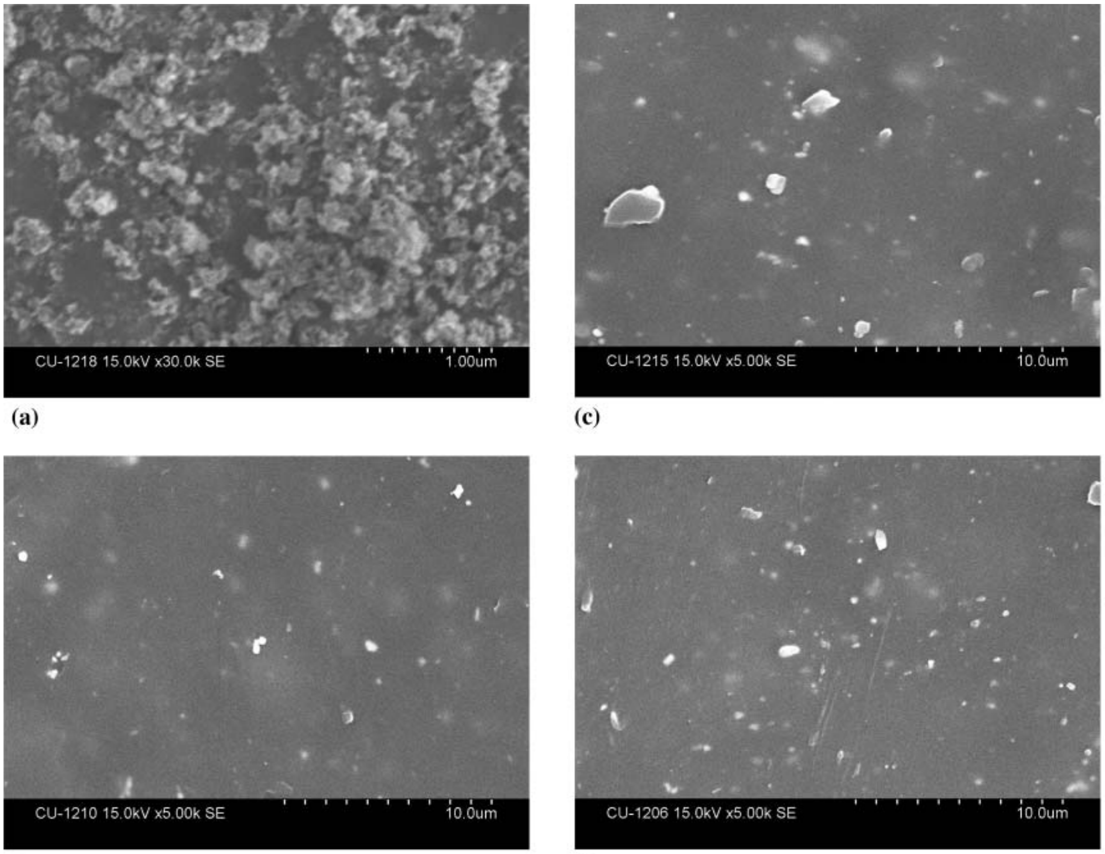

(a) **(c)** **(b)** **(d)**

Fig. 6. (a) SEM micrograph of nano-alumina at high magnification (magnification = 30,000X), **(b)** SEM micrograph of unfilled (Gum) natural rubber compound, taken at a magnification of 5,000X, **(c)** SEM micrograph of 20 phr active alumina loading natural rubber composite, taking at a magnification of 5,000X, **(d)** SEM micrograph of 20 phr nano alumina loading natural rubber composite, taking at a magnification of 5,000X.

is the oxidation resistance due to very thin alumina film formation on aged samples (29). Thin film formation depends on the size of alumina particles. Smaller free particles (in nano alumina) can easily diffuse and migrate to the surface.

3.10 Morphology

SEM micrograph of nano- alumina at high magnification (30,000X) is shown in Figure 6(a). The nano-alumina sample seems to have a large surface area. Some are found to be in agglomerated form.

Figures 6(b), 6(c) and 6(d) display SEM micrograph for unfilled, active alumina filled and nano- alumina filled natural rubber composites at magnification of 5,000X, respectively. Both active and nano fillers uniformly distributed. It can be observed that the density of agglomerates is greater in active alumina composite than nano composite.

4 Conclusions

With the help of the reported experiments on different sizes of alumina-filler particles, it has been possible to evaluate cure characteristics, kinetics of vulcanization, crosslink density, mechanical properties and oxidative aging behavior of ENR compatibilized filled natural rubber vulcanizates in a comprehensive way.

As expected, incorporation of alumina filler in natural rubber increased viscosity, stiffness and network chains within the composites. However, nano alumina influenced these properties to a great extent in comparison to other types of alumina. Curing characteristics like scorch time and optimum cure time were found delayed. This is opposite to that for ZnO-rubber composite. Nano-alumina particles' effect was more significant than others. Kinetics of vulcanization for all alumina filled composites were first order. Specific rate constant was lowest for nano composite. Thus, natural rubber–nano alumina composite shows strong interaction in the presence of ENR, which is evident from crosslink density value.

All the composites showed substantial improvement in their mechanical properties. In comparison to unfilled rubber compound, nano alumina composite shows 147% increase in modulus and 190% increase in ultimate tensile strength, while 20% decrease in elongation at break. Some improvement in the hardness was observed in nano-alumina composite in comparison to others.

The most significant result for nano alumina composite was found to be its very high oxidative resistance behavior. These findings have a great practical importance for rubber compound development.

Morphology of alumina rubber composite fracture surfaces shows that fillers are uniformly distributed and hinder the chain movement during deformation.

References

1. Zhang, Q., Tian, M., Wu, Y., Lin, G. and Zhang, L.(2004) *J. of Appl. Poly. Sci.*, 94(6), 2341–2364.
2. Wang, Y., Zhang, H., Wu, Y., Yang, J. and Zhang, L. (2005) *J. of Appl. Poly. Sci.,* 96(2), 318–323.
3. Mishra, S. and Shimpi, N.G. (2005) *J. of Appl. Poly. Sci.*, 98(6), 2563–2571.
4. Gilbert, E.N., Hayes, B.S. and Seferis, J.C. (2003) *Poly. Engg. & Sci.*, 63(5), 1096–1104.
5. Leuteritz, A., Kretzschmar, B., Pospiech, D., Costa, F.R., Wagenknecht, U., Heinrich, G. In Polymeric Nanostructures and their Applications, Nalwa, H.S., Ed. American Scientific Publications: California, Vol. 2, 120–125, 2007.
6. Yusoff, M.S.M. and Masliana, M. (2007) *The Malaysian J. of Analy. Sci.*, 11(1), 262–268.
7. Silvernall, W.L. In Kirk Othmer Encyclopedia of Chemical Technology, 3rd Ed., Editor: Grayson, M, Willy Interscience Publications: New York, Vol. 5, 299, 1979.
8. Choi, S.S. (2000) *J. of Appl. Poly. Sci.*, 75(11), 1378–1384.
9. Teh, P.L., Ishak, Z. A.M., Hashim,A.S., Kocsis, J.K. and Ishiaku, U.S. (2004) Euro. Poly. J., 40, 2513- 2521.
10. Morrel, S.H. In Rubber Technology and Manufacture, 2nd Ed., Blow, C.M. and Hepburn, C., Eds. Butterworths: London, 189, 1987.
11. Ishak, Z.A.M. and Bakar, A.A. (1995) *Euro. Poly. J.*, 31(3), 259–269.
12. Ciprari, D.L. Master Thesis, (2004) Georgia Institue of Technology.
13. Aprem, A.S., Joseph, K., Mathew, T., Altstead, V. and Thomas, S. (2003) *Euro. Poly. J.*, 39(7), 1461–1466.
14. Peter, J., Nieuwenhuizon, S.T., Jaap, G.H., Spek, A.L. and Reedijk, J. (2006) *Chemistry-A, Euro. J.*, 11, 1846–1857.
15. Barlow, F.W. In Rubber Compounding, Principles, Materials And Technology, 2^{nd} Ed., Google book, 104–106, 1993.
16. Wang, P.Y., Chen, Y. and Qian, H.L. (2007) *J. of Appl. Poly. Sci.*, 106(6), 3255–3259; Arrillaga, A., Zaldua, A.M., Atxurra, R.M. and Farid, A.S. (2007*) Euro. Poly. J.*, 43(11), 4783–4799.
17. Zhao, F., Shi, X. and Zhang, P. (2009) *J. Macromolecular Sci. Part B*, 48(4), 663–669.
18. Huisin, G., and Nongyue, H. In Polymeric Nano Structure and there Applications, Nalwa, H.S., Ed. American Scientific Publishers: California, Vol. 2, 367, 2007.
19. Duong D. Do., Adsorption Analysis; Equilibria and Kinetics, Series on Chem. Eng. Vol. 2, Imperial College Press, London, 25, 1998.
20. Sangwichien, C., Sumantrakool, P. and Patarapaiboolchai, O. (2008) *Chiang. Mai. J. Sci.*, 35(1), 141–149.
21. Heinrich, G., Kliippel, M. and Vilgis, T.A.(2002) *Current Opinion in Solid State and Materials Science*, 6(3), 195–203.
22. Treloor, L.R.G. In The Physics of Rubber Elasticity, Oxford Classic Texts, Oxford University Press: Oxford, 131, 2005.
23. Mark, J.E. (1994) *J. of Inorganic and Organometallic Polymers*, 4(1), 31–44.
24. Cai, J.J. and Solovey, R. (1999) *J. of Material Sci.*, 34(19), 4719–4726.
25. Bokobza, L., Garnaul, G. and Mark, J.E. (2002) *Chem. Mater.*, 14(1), 162–167.
26. Mohamad, N., Muchtar, A., Ghazali, M.J., Hj. D. and Azhari, M.C. (2008) *Euro. J. of Scientific Research*, 24(4), 538–547.
27. MeorYusoff, M.S. and Muslimin, M. (2007) *The Malaysian J. of Analytical Sciences* 11(1), 262–268.
28. Bokobza, L. (2007) *Polymer*, 48(17), 4907–4920.
29. Hamed, G.R. and Zhao, J. (1999) *Rubb. Chem. and Technol.*, 72, 721–729.